REVIEW ON ALKALI VAPOR CHARGE EXCHANGE CANALS FOR HE^- AND HIAF ALPHA INJECTOR

https://hiaf.anu.edu.au/

Nikolai Lobanov, Peter Linardakis, Thomas Kitchen, Thomas Tunningley, Mark Gwyneth and Daniel Tempra

Australian National University

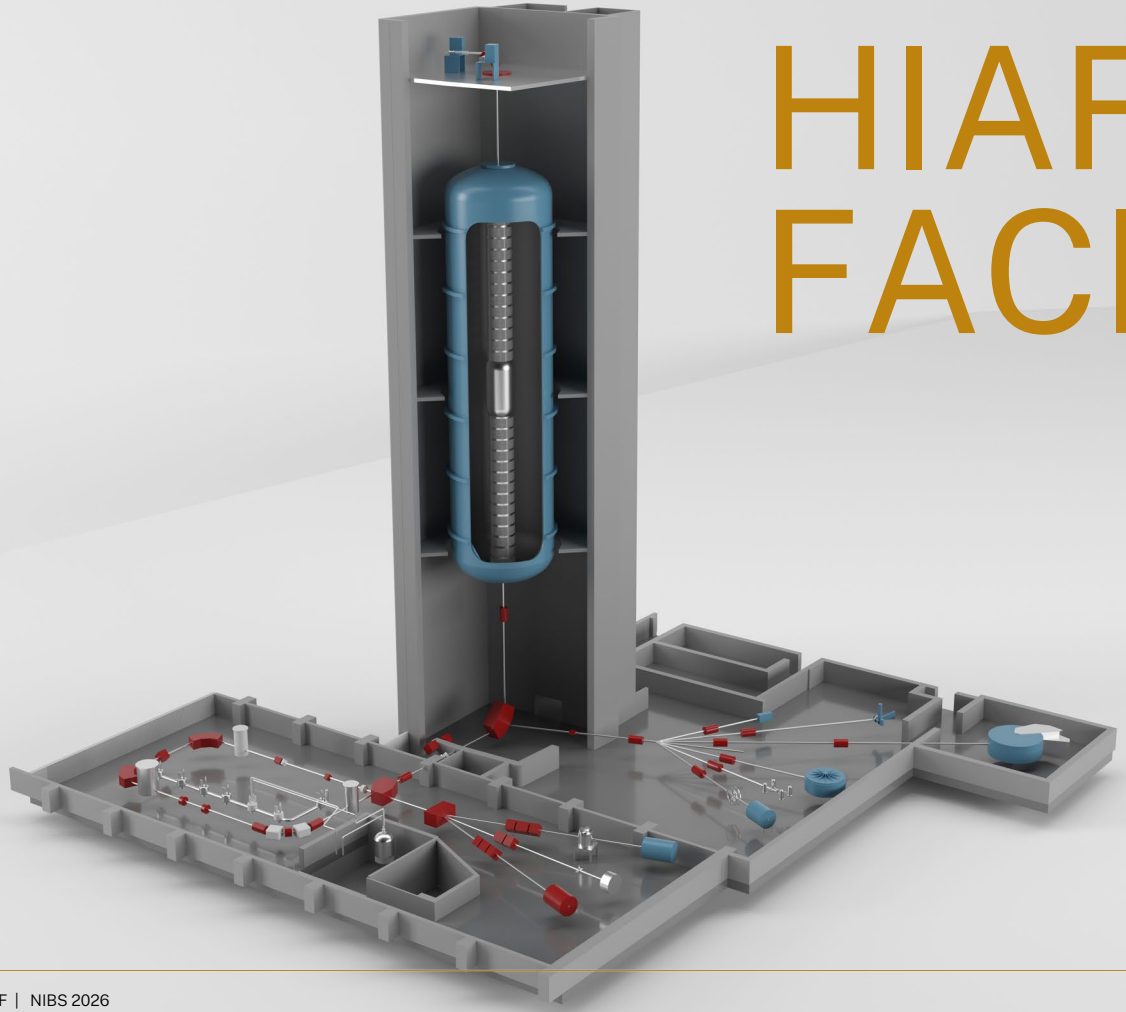
Department Nuclear Physics and Accelerator Applications, ANU, Canberra, Australia



Trevor Dickinson
www.trevordickinson.com

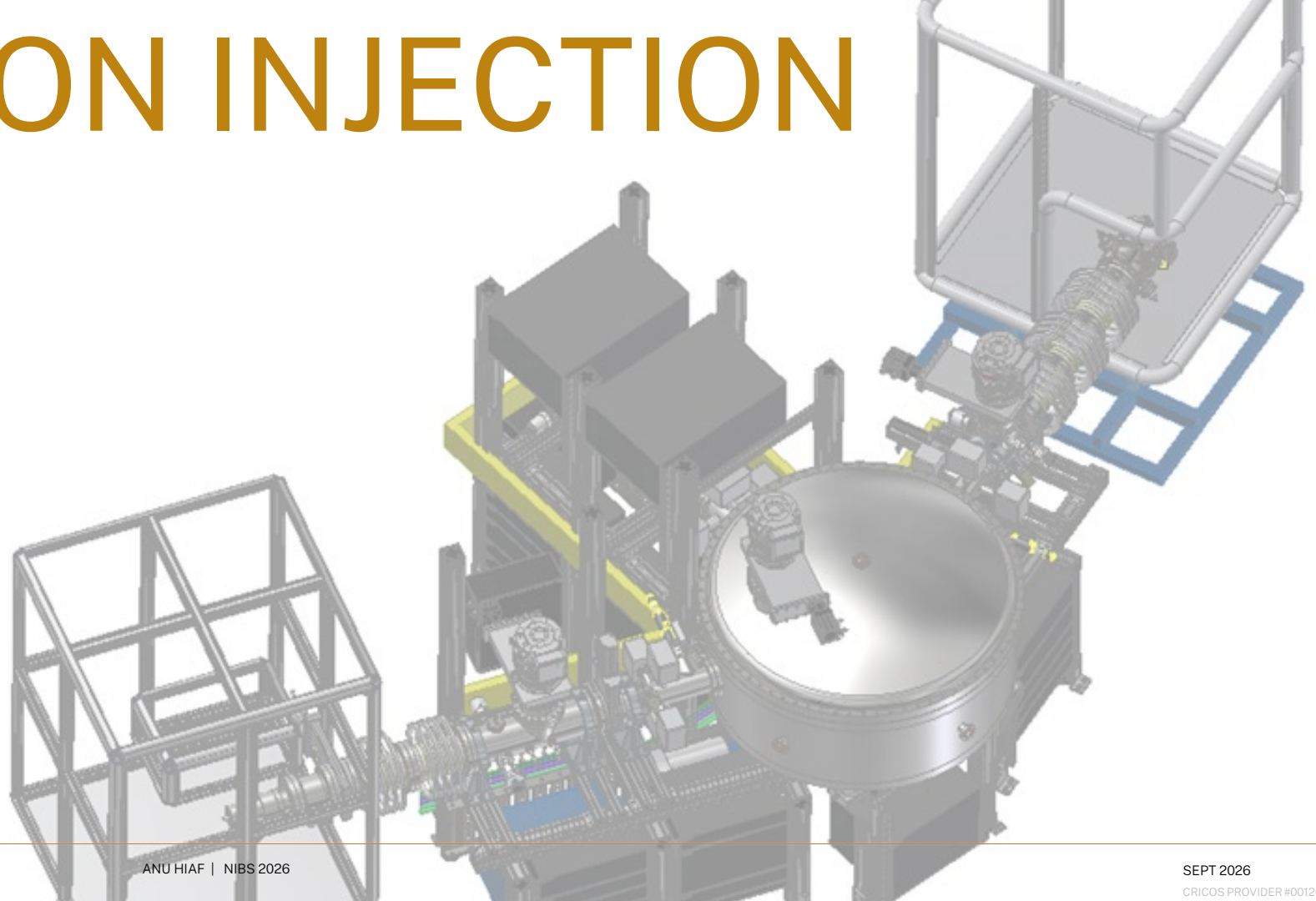
CRICOS PROVIDER #00120C

HIAF FACILITY



CRICOS PROVIDER #00120C

ION INJECTION



CRICOS PROVIDER #00120C

The Alpha Injector Project

Installation of a new ion source to produce negative helium ions (ECR/RF/DUOPLASMATRON/Rb CEC ion source)

Installation of a new 110° electrostatic analyser (ESA)

Repositioning the existing multi-cathode MSNICS ion source to integrate with the ESA

Plus additional associated work

Installation of new safety cages around all three ion sources

Reconfiguration and upgrade of the high-voltage functional safety interlock system

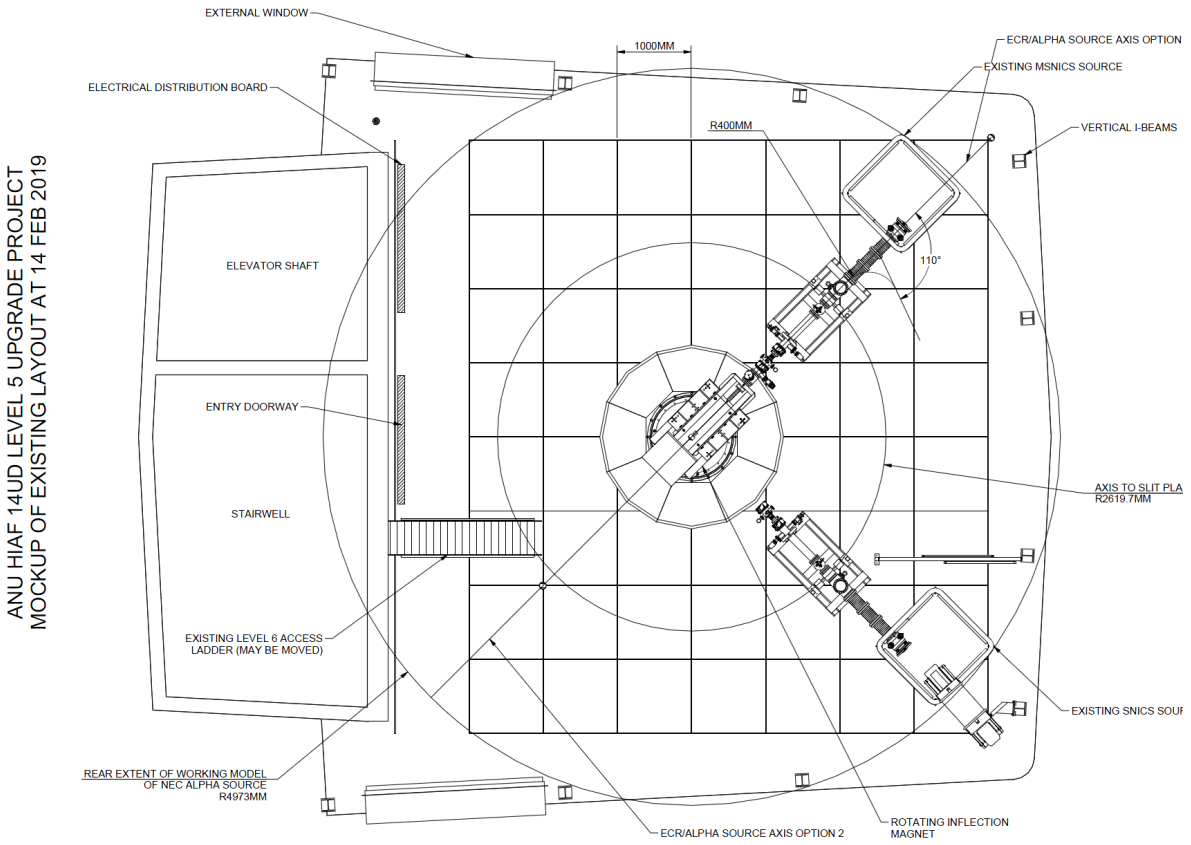
Motivation

The sensitivity of AMS for heavier nuclide detection is currently constrained by high backgrounds from neighbouring isotopes due to low- and high-energy tails Electrostatic Analyser

Users are demanding 3He and 4He (alpha particles) for research problems New negative He ion (alpha) source

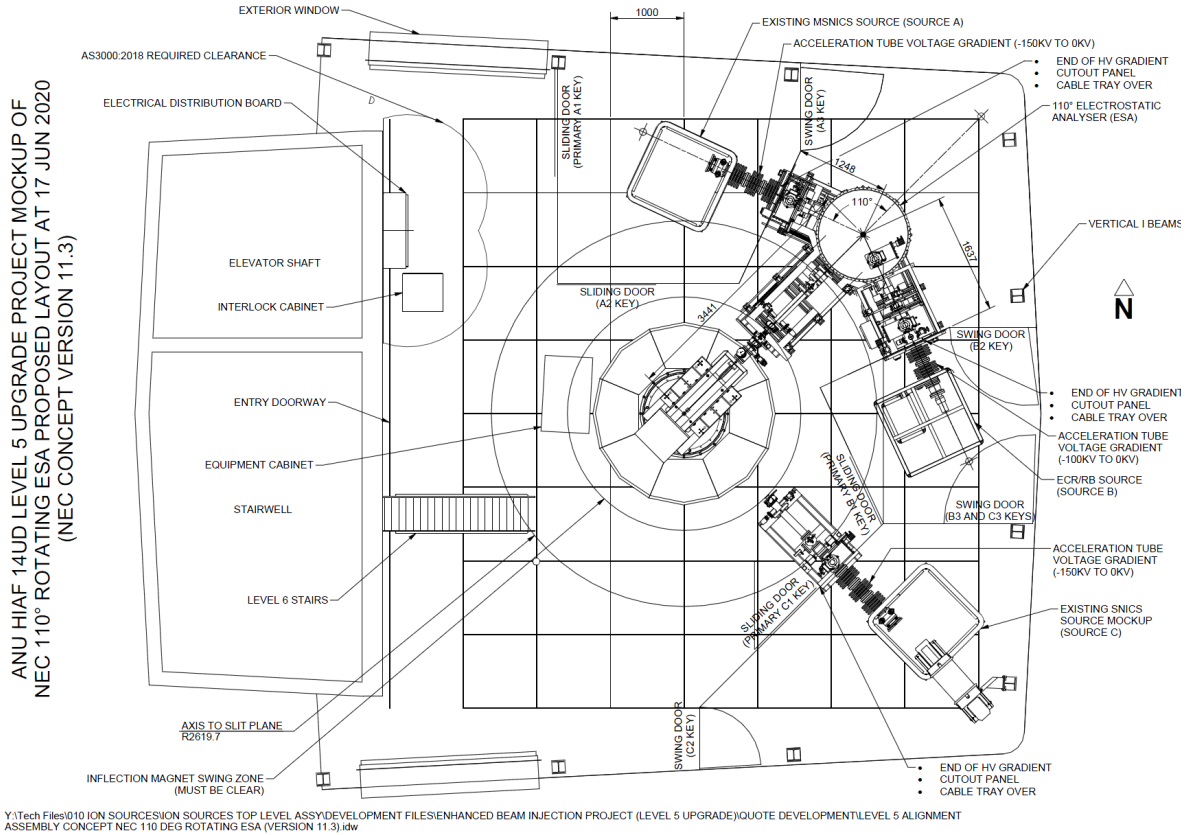
CRICOS PROVIDER #00120C

Existing layout



CRICOS PROVIDER #00120C

Planned layout



CRICOS PROVIDER #00120C

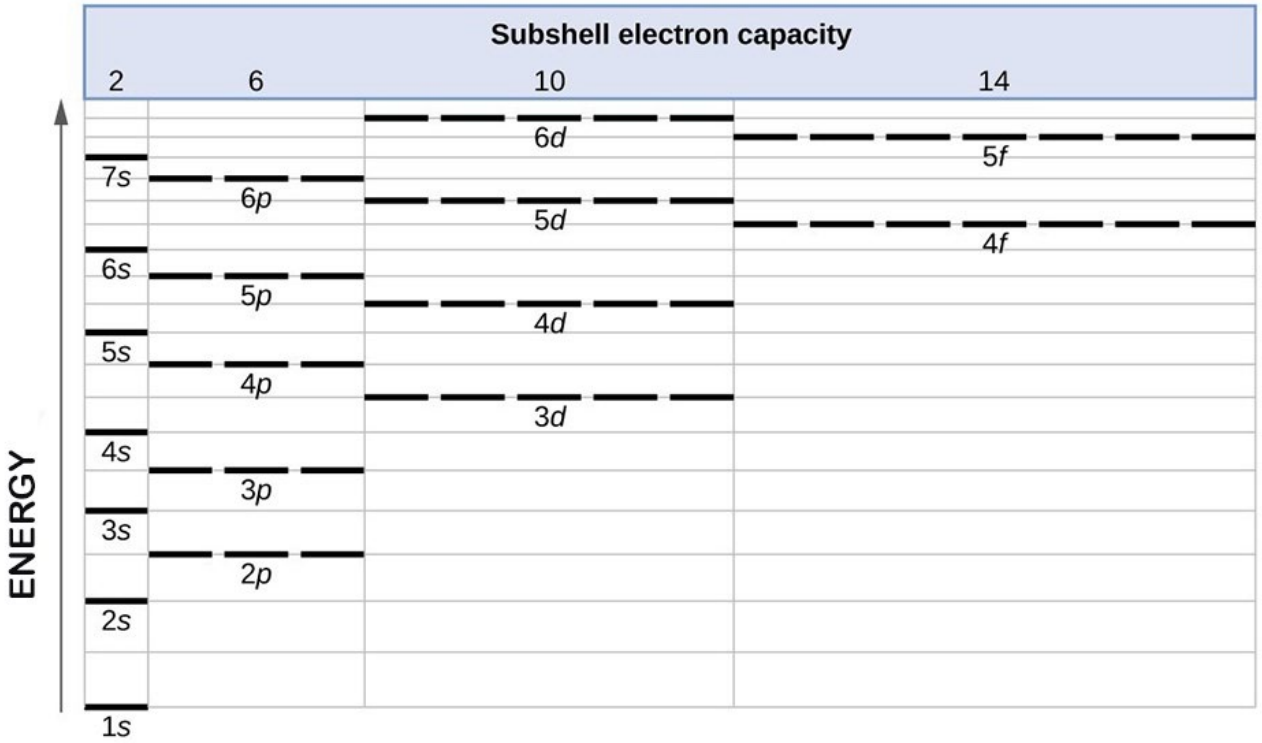


National Electrostatics Corporation

Courtesy NEC

CRICOS PROVIDER #00120C

The Fundamentals of He^- Beam Formation



Format of atomic term symbols: $^{2S+1}L_J$ L is total orbital angular momentum (upper case from s, p, d, f, g, h, ...,) L=0 ➡ S; L=1 ➡ P

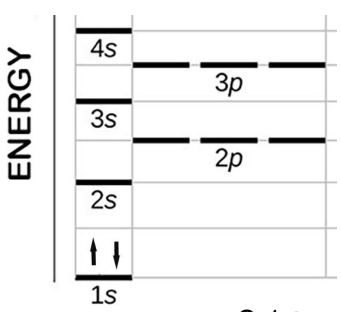
S is total spin quantum number;
J=L+S is total angular momentum
2S+1 is spin multiplicity

Singlet He* state $^1S_0$:
2S+1 = 1 (singlet)
Electron spin S= ½-½= 0;
J= 0+0 = 0

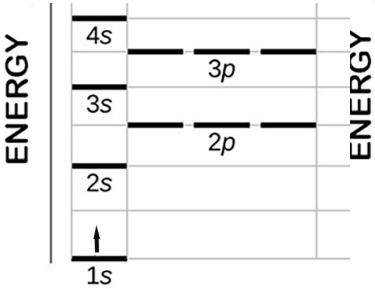
Triplet He* state $^3S_1$:
2S+1 = 3 (triplet)
S= ½+½= 1; 2S+1= 3;
J= L+S= 0+1= 1

CRICOS PROVIDER #00120C

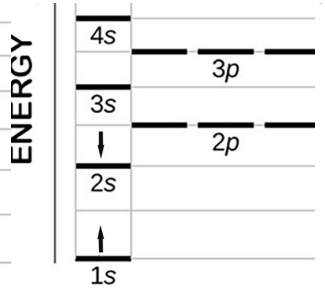
The Fundamentals of He^- Beam Formation: Energy Box Diagrams



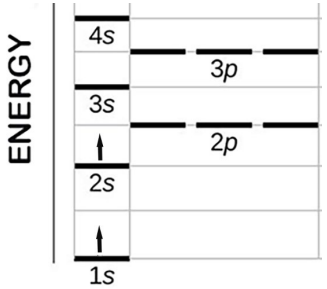
He ground level $1s^2\ ^1S_0$



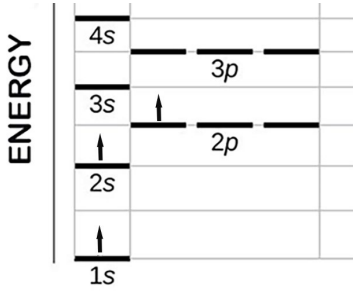
$He^+\ 1s^1\ ^2S_{1/2}$



He* singlet $1s^1 2s^1\ ^1S_0$

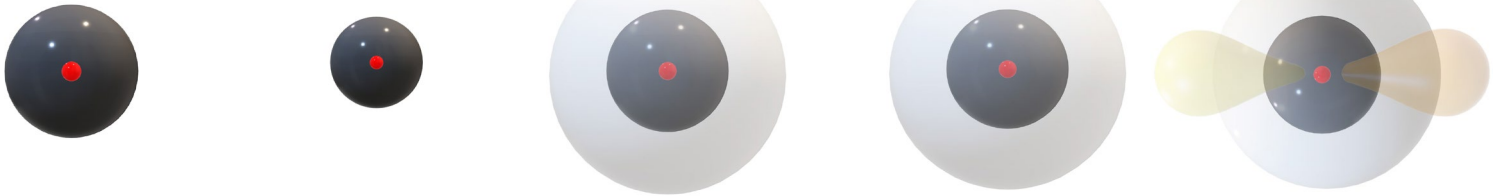


He* triplet $^3S_1$



He^- quartet $^4P_{5/2}$

3-D e^- probability clouds (orbitals)



Total Spin S	½ - ½ =0	½	0	½ + ½ =1	½ + ½ +½ =3/2
Orbit. Moment. L	0	0	0	0	1
Angular Moment. J	0	1/2	0	1	5/2
Lifetime	indefinitely stable	indefinitely stable	19.7 ms	7800 sec	350 µs

CRICOS PROVIDER #00120C

Key Quantum Mechanical Features of He

He ground level $1s^2\ {}^1S_0$

No orbital vacancy in core 1s shell accommodating two e^- with ↑↓ spin (Pauli exclusion principle); extreme chemical inertness E_{i1}=24.59 eV; Absolute bottom 0 eV on He Grotrian diagram; $R_{at/ion}$=31 pm



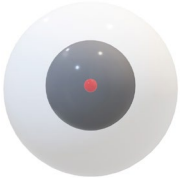
He^+ doublet $1s^1\ {}^2S_{1/2}$

Only one 1s orbital e^- against 2 nuclear protons, atom shrinks H-like atom described by Bohr's or Schrodinger formulas; Massive Binding Energy E_{i2}=54.42 eV and volume contraction



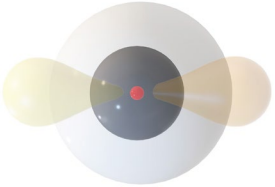
He* singlet ${}^1S_0$ and triplet ${}^3S_1$

Only two e^- creates para/ortho separation; Parahelium energy is 20.61 eV; Orthohelium is lowest energy excited state 19.82 eV (Hund's Rule) since ↑↑ spin causes e^- stay further apart



He^- quartet ${}^4P_{5/2}$

Hund's Rule and ↑↑ spins keep e^- spatially separated to minimize Coulomb repulsion; Vacant 1s shell with missing e^- acts as energy trap allowing eventual auto-ionization; 2s and 2p e^- are far from nucleus and shielded by 1s e^-, He^- ion is large $R_{at/ion}$=250-320 pm due to shell jump, e^- shielding and ↑↑ spin repulsion; Functions like alkali metal atom.

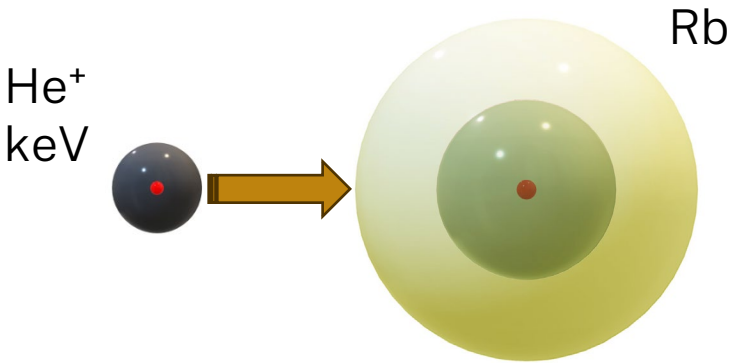


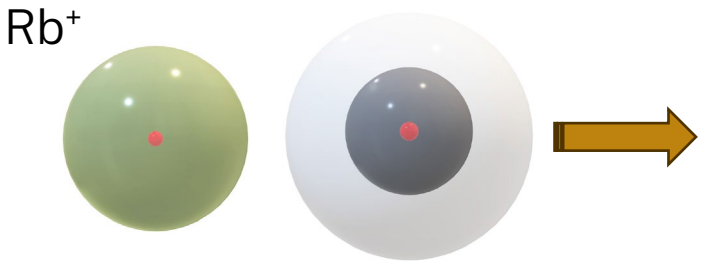
CRICOS PROVIDER #00120C

Production of He^- via charge exchange

The production of He^- relies on two sequential charge-exchange reactions:

A. $He^+ + Rb \rightarrow He^* \text{ (triplet)} + Rb^+$ **triplet production**





He* balloons by ~500% shifting from single to pair of concentric spheres

Rb electron configuration (A=37) is $1s^2 2s^2 2p^6 3s^2 3p^6 4s^2 3d^{10} 4p^6 5s^1$, or $[Kr]5s^1$ in noble gas shorthand notation

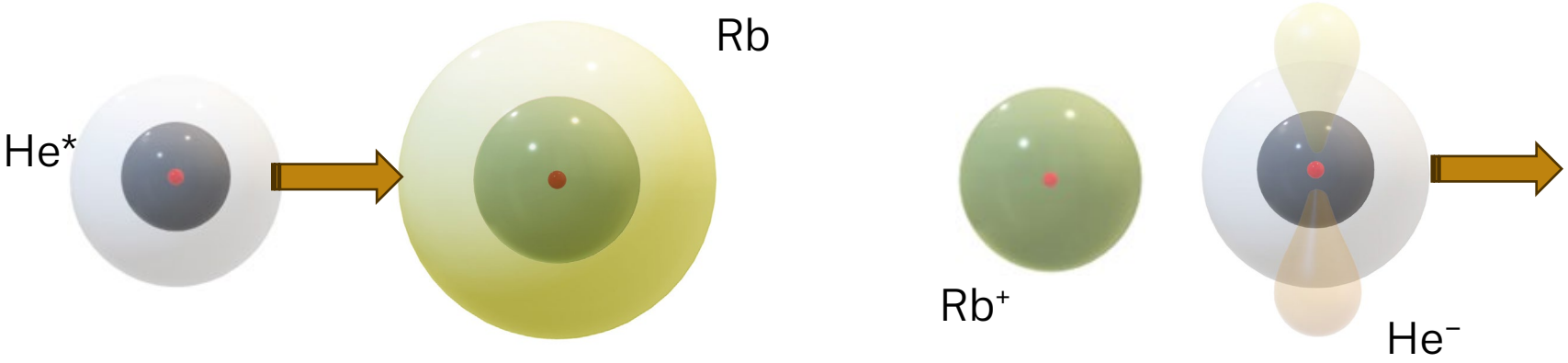
He^+ approaches Rb at high-speed sweeping through 5s e^- cloud; He nuclear charge +2 exerts electrostatic pull on Rb weakly bound 5s e^-.

The e^- jumps across gap deserting Rb atom.

CRICOS PROVIDER #00120C

Production of He^- via charge exchange

B. $He^* + Rb \rightarrow He^-(quartet) + Rb^+$ **negative He ion production**



Rb collapses losing giant loosely bound 5s envelope. Remaining 36 e^- form spherical Kr-like core.

Composite of two spheres intersected by dumbbell shaped cloud

CRICOS PROVIDER #00120C

Production of He^- via charge exchange: semi-classic cross section

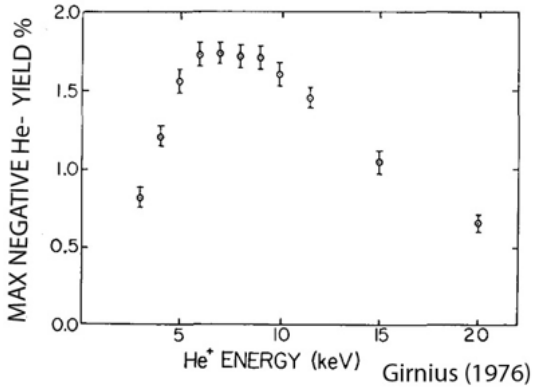
Cross-section σ depends on velocity *v* of He^+ and energy mismatch ΔE between initial and final states

$$\sigma(v) \approx \pi \cdot R_c^2 \cdot f(v, \Delta E)$$

πR_c^2 is area of circle where R_c is critical internuclear distance where electronic wave functions of He^+ and Rb significantly overlap. Rb has massive 5s cloud so R_c and σ_{+*} are large.

Velocity Matrix Function f(v, ΔE) scales according Massey Criterion
ΔE is energy defect, *a* is effective interaction range ~ size of e^- cloud, *h* is Planck's constant

$$\gamma = \frac{\Delta E \cdot a}{\hbar \cdot v}$$



For He* + Rb → He^- + Rb^+ ΔE is difference between energy released when triplet He* becomes He^- (~0.07 eV) and ionization energy of Rb (4.18 eV). This leaves small mismatch of ~ -4.1 eV

Because ΔE is small, near resonance, σ has got Massey peak at γ ~1. He* travel time to cross interaction zone *(a/v)* matches quantum transition time of e^- ($h/\Delta E$)

CRICOS PROVIDER #00120C

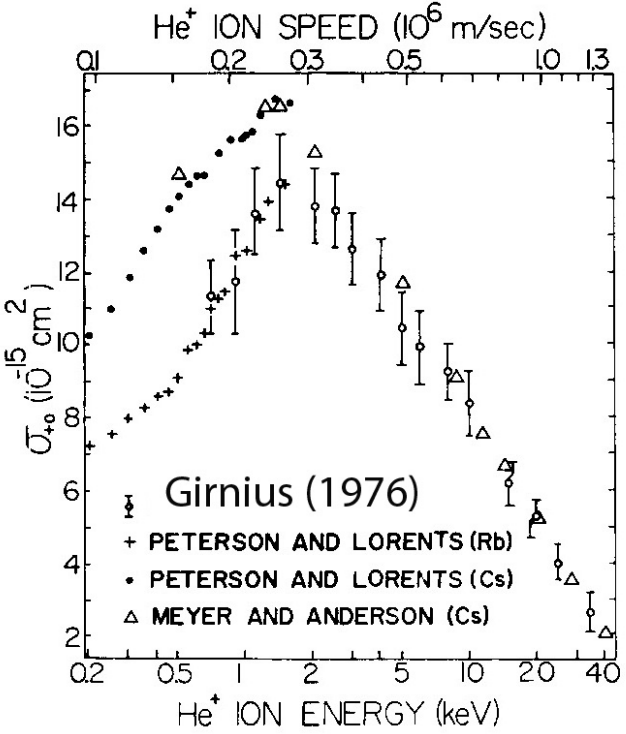
Optimizing Ion Source for Enhanced Beam Generation: *Beam Injection Energy*

Low energies (~1.5 keV): electron detachment from He^- becomes highly probable, while increased beam scattering and geometric spreading reduce overall efficiency.

Intermediate energies (3–7 keV); the charge-exchange cross section is relatively large, enabling more efficient collisions, enhanced production of metastable He* atoms, and a greater likelihood of the secondary collision required for He^- formation

At> ~7 keV He^- yield decreases since charge-exchange cross section σ_{+0} declines, resulting in fewer He* atoms and a lower probability of secondary collisions due to shorter interaction time.

Direct ionization of Rb by He^+ becomes more significant at these energies as per $He^+ + Rb \rightarrow He^+ + Rb^+ + e^-$



cross section σ_{+0} for $He^+ + Rb \rightarrow He^0 + Rb^+$

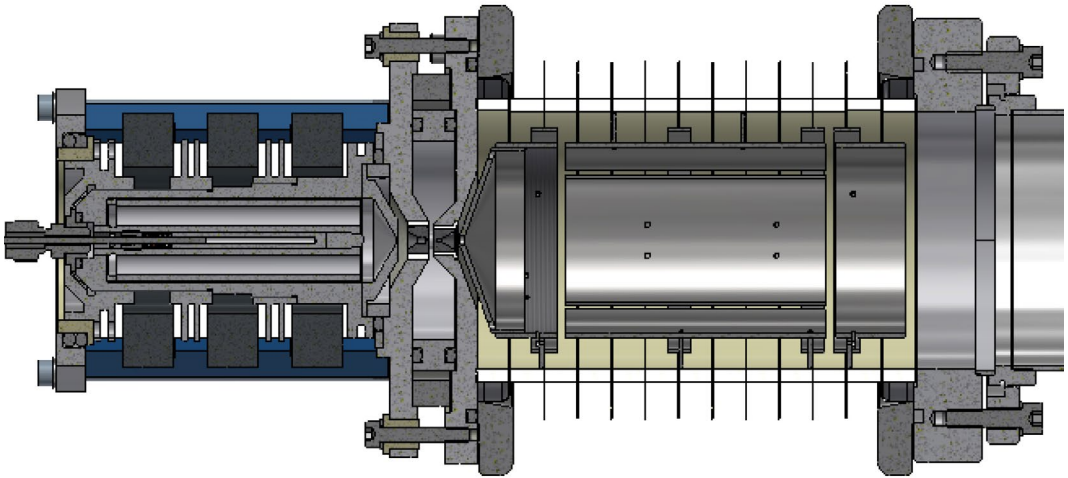
CRICOS PROVIDER #00120C

Optimizing Ion Source: *IS Performance Considerations and Influence of Gas Flow and Source Pressure*

Important parameters include arc current and discharge voltage, electron temperature and plasma density, cathode emission characteristics, plasma confinement efficiency and discharge stability over extended operation.

Maximizing He^+ current while minimizing vacuum loading with suitable ion source designs, such as multicusp sources with magnetic confinement or duoplasmatron sources.

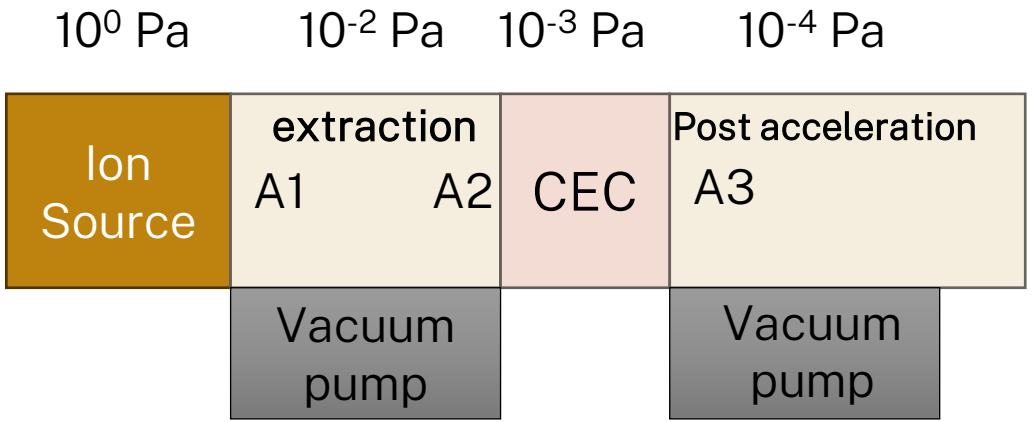
ANU duoplasmatron with permanent magnets ,
100 µA He+ at 300 mA discharge current,
2.6×10^{-4} Pa in extraction region with 170 l/s turbo



CRICOS PROVIDER #00120C

Vacuum Engineering Requirements for Efficient Negative-Ion Production

Combination of high He^+ beam intensity and low beam energy results in ion beam transport influenced by space charge. Optimal background pressure to compensate space-charge forces is in ~10^{-4} mbar range. Pressure after CEC should be as low as possible to reduce neutralization loss of He^-. A differentially pumped system comprises three vacuum stages, each with an approximate tenfold pressure reduction.



Apertures

A1~ 0.5 mm

A2,3~ 5-7 mm

CRICOS PROVIDER #00120C

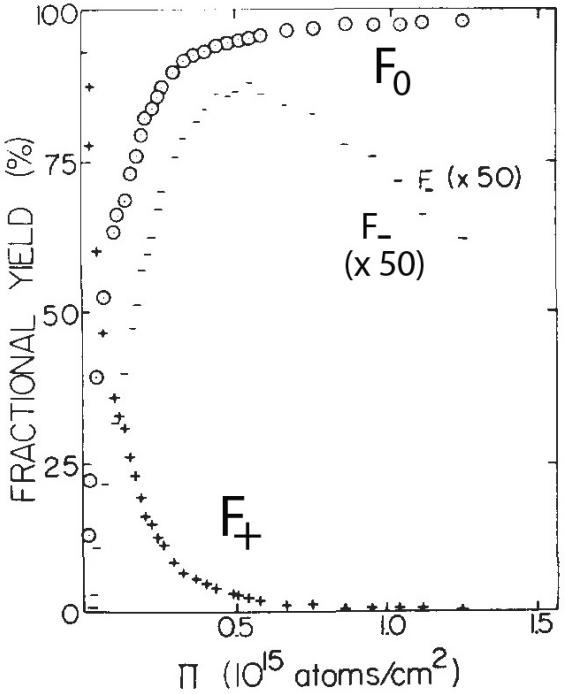
Alkali-Based Charge Exchange; Key Parameters and Challenges: *Target Thickness*

The He^- fraction (F^-) depends on alkali target thickness (π, atoms/cm^2), increasing to a maximum before declining. For a Rb target, the peak occurs at (5–7) × 10^{14} atoms/cm^2.

At low π ⟹ inefficient production of excited helium atoms (He^{0*}).

At the optimum π ⟹ sufficient collisions occur to produce He^{0*} efficiently and convert it to He^-, while minimizing losses due to collisional destruction.

At greater π ⟹ increased collisions deactivate excited states and reduce the regeneration of metastable intermediates. He^- ions may be neutralized through electron stripping in subsequent collisions.



He on Rb at 7 keV Girnius(1976)

CRICOS PROVIDER #00120C

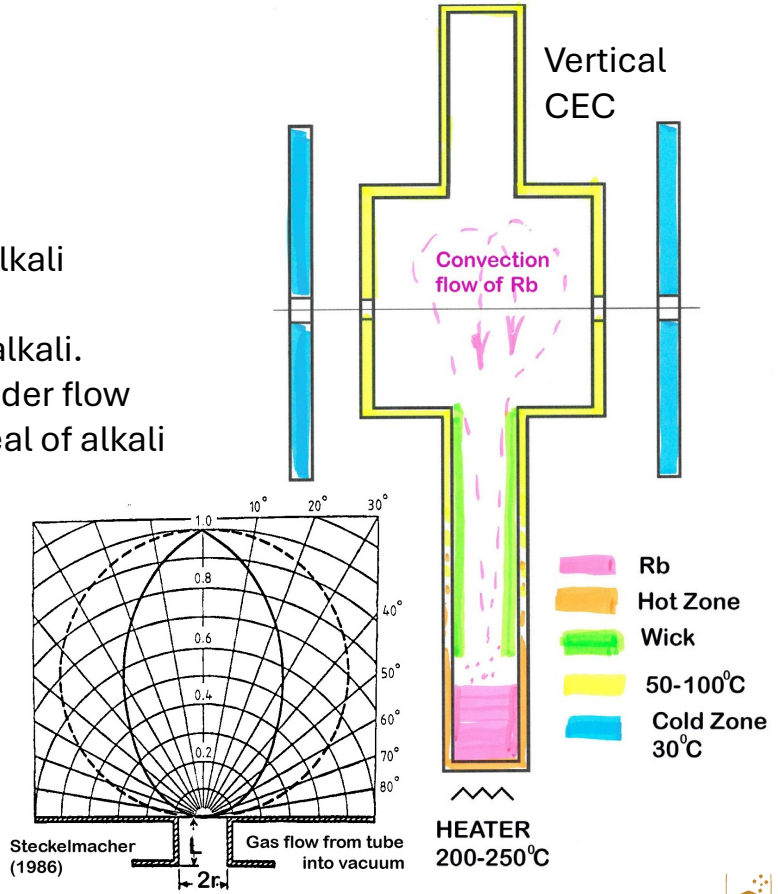
Alkali-Based Charge Exchange: *Charge-Exchange Cell Design Considerations*

CECs operate in horizontal or vertical configurations. Typical CEC has a length of ~50-100 mm exchange region with small entrance/exit apertures (~5-7 mm).

The typical CEC features: better localization of alkali vapor; shielded insulators. The assembly can be sealed/removed *in situ* without oxidation of the alkali. Alkali is introduced using hypodermic syringe under flow of argon. Mechanical feed-through breaks the seal of alkali ingot under a vacuum .

Cs level device is based on measuring the resistance of a high resistivity electrode immersed in the liquid Cs.

Density of alkali vapors along the ion beam path and π are determined considering oven as a Knudsen effusion cell, the angular distribution of Cs flow and the oven transmission factor.



CRICOS PROVIDER #00120C

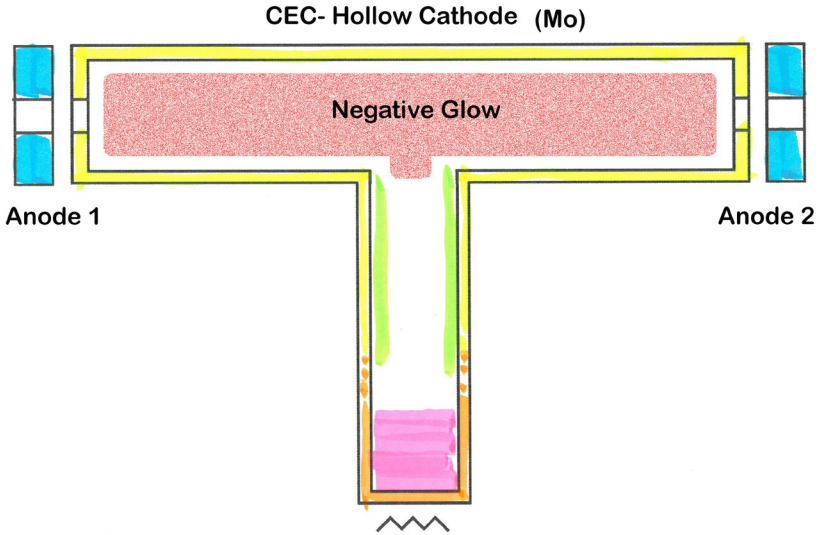
Alkali-Based Charge Exchange: *Alkali Temperature and Thermal Management*

CEC maintains thermal gradients, promote alkali vapor circulation, and facilitate condensate return. Capillary recycling system incorporating wick within the canal captures condensed alkali vapor, converts it back to liquid metal, and returns it to the heated region via capillary action.

Light-Induced Atomic Desorption (LIAD) used as a non-thermal control of rubidium vapor density at ~ 10^{-5} Torr in Spin-Exchange Relaxation-Free (SERF) magnetometers.

Controlling alkali vapor density using hollow cathode (HC) effect. Advantages: (a) rapid control of vapor density, (b) improved alkali retention, and (c) enhanced recycling of alkali adsorbed on molybdenum surfaces.

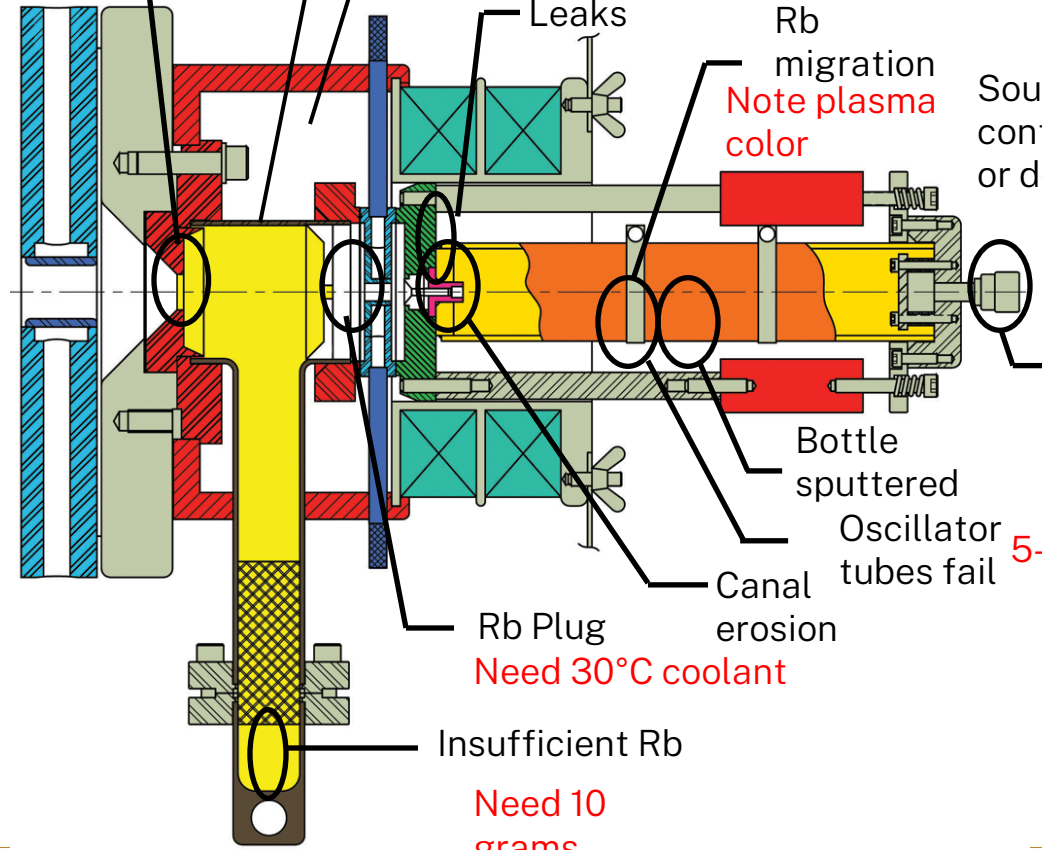
Risks: plasma induced contamination; plasma could alter beam emittance and charge exchange efficiency.



CRICOS PROVIDER #00120C

NEC report to SNEAP 2008 (ANU) And 50th SNEAP 2016 (ANSTO)

Rb M.P. = 38.9° C
V.P. = 0.1 Torr (13.3 Pa)
Oven = 200° - 250° C
Air = 50° C
Liquid = 30° C

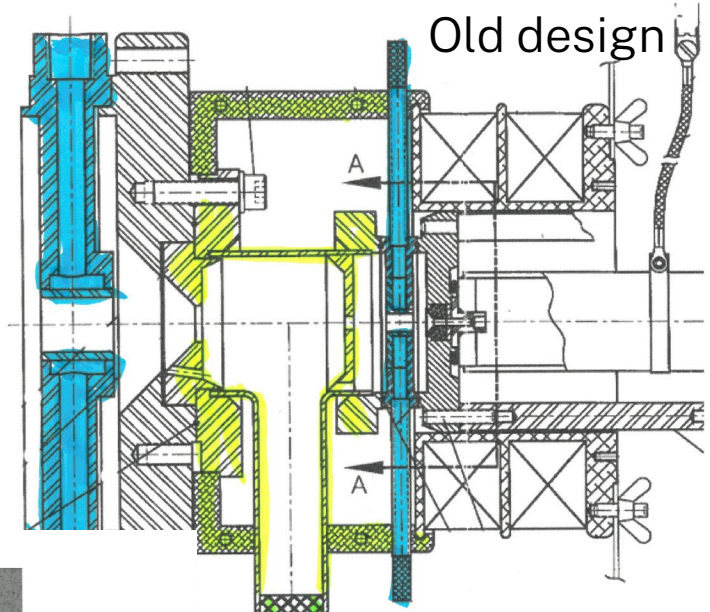


CRICOS PROVIDER #00120C

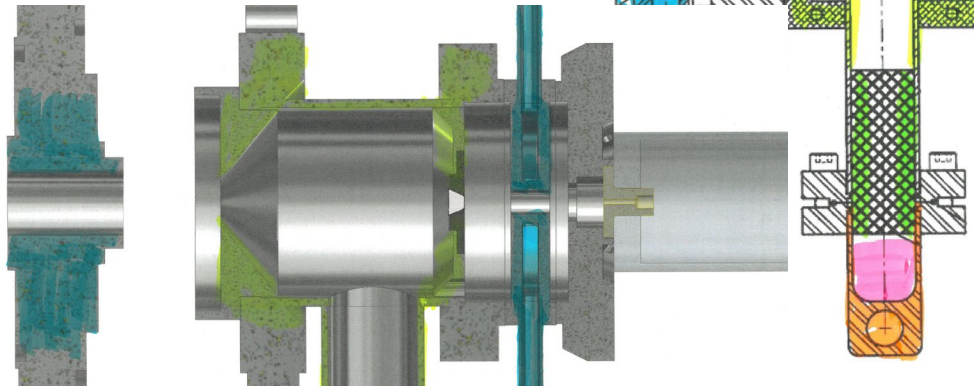
Charge-Exchange Cell Design Considerations: ANU Perspectives

- Partition plenum around Rb chamber
- Chamber entrance aperture wear & shape
- Chamber exit aperture size and shape
- Bottle rigidity
- Temperature control of Rb oven
- G size remote Helium cylinder
- Don’t use return wick?
- Excessive Rb migration toward RF tube?
- H_2 leak chase after each rebuild
- Outgas RF bottle before loading Rb
- Don’t turn it off!

Old design

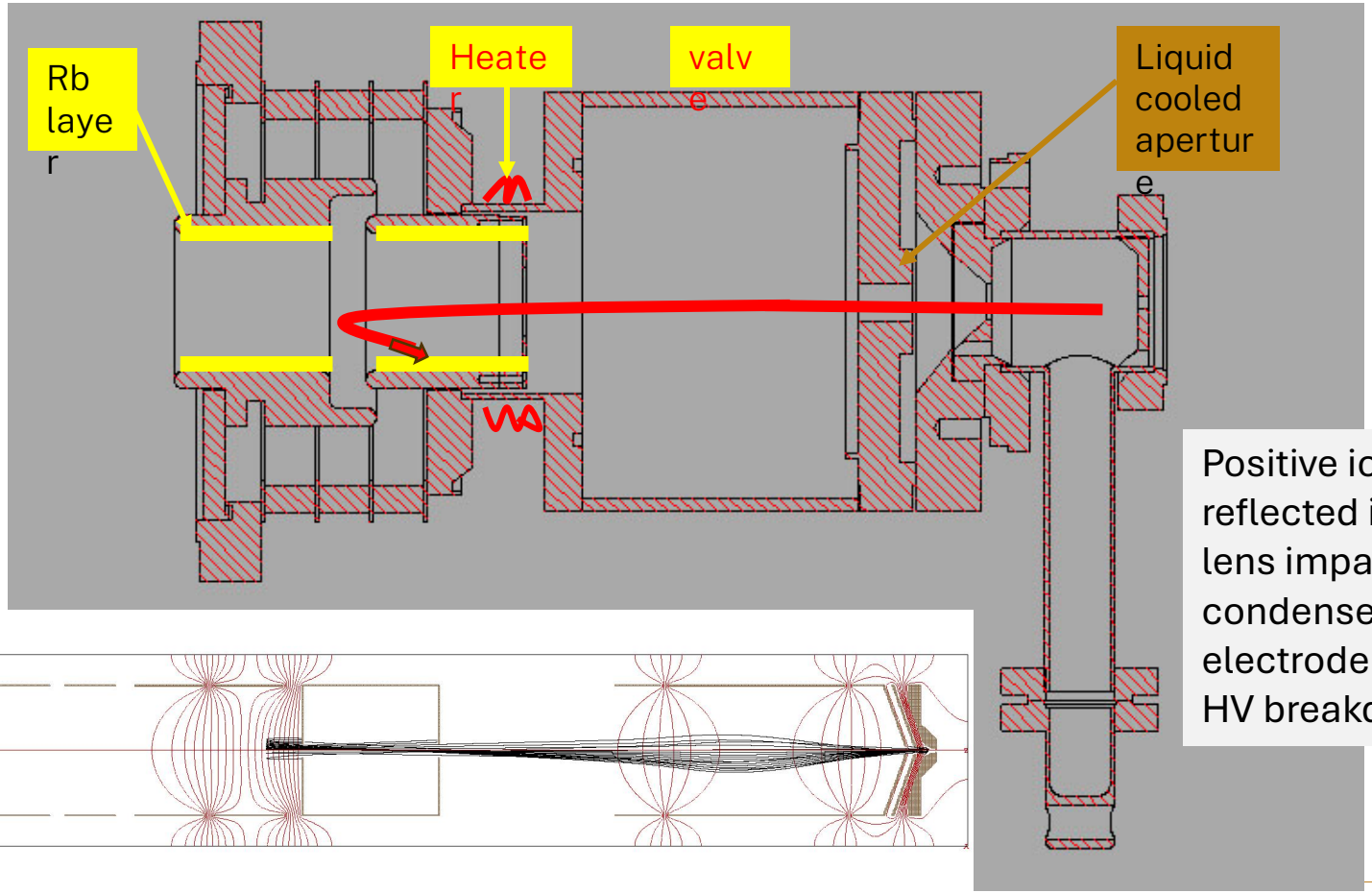


New design
circa 2011





CRICOS PROVIDER #00120C

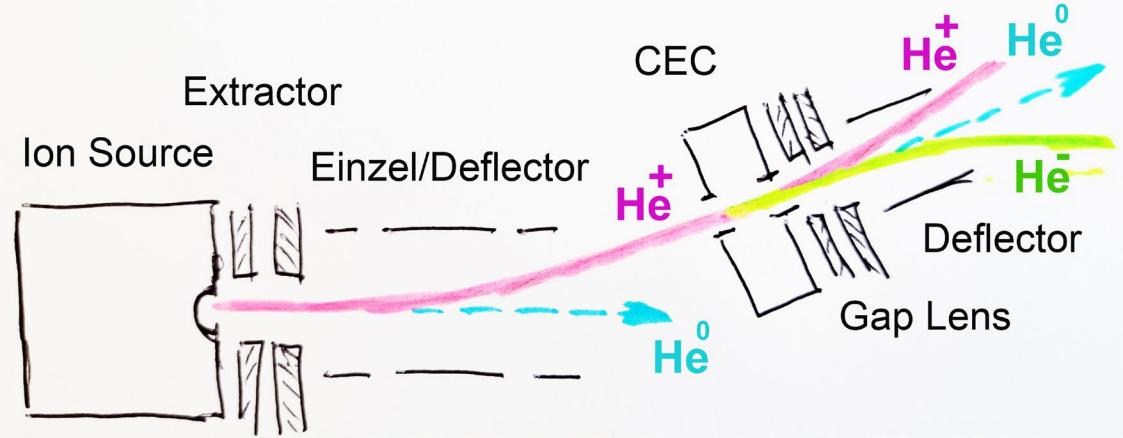


Positive ions reflected in gap lens impact on Rb condensed on electrode causing HV breakdown

Beam Transport and Emittance Considerations

Lens system provides beam deflection that prevents alkali contamination and blocks plasma/neutral flux entering the CEC.

To prevent intra-beam stripping, the He^- beam must be separated from the more intense He^+ and He^0 beams using deflector positioned downstream of the CEC.



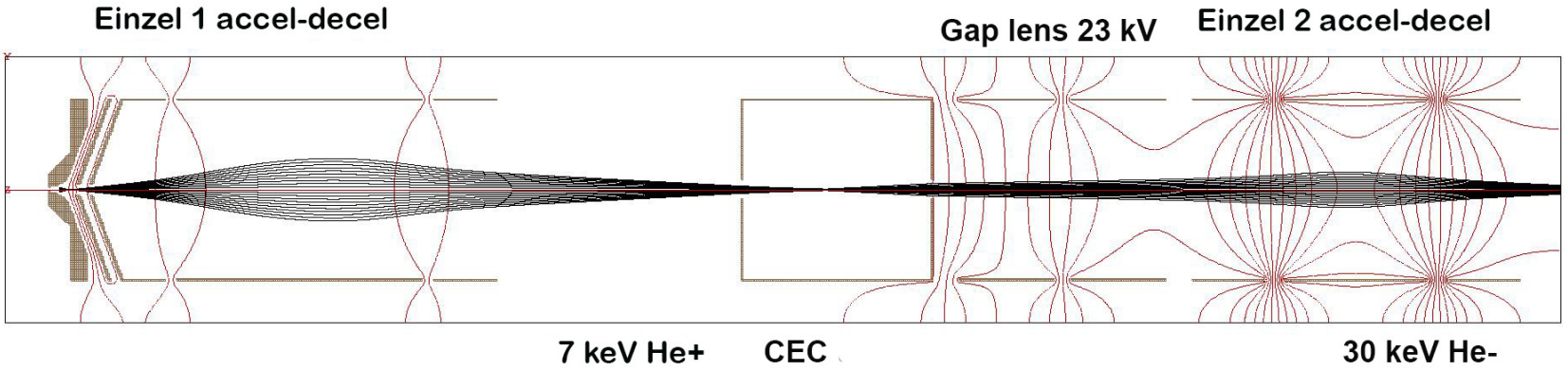
ε_n for 100 μA RF He^+ ion source is ~0.2 π mm mrad.

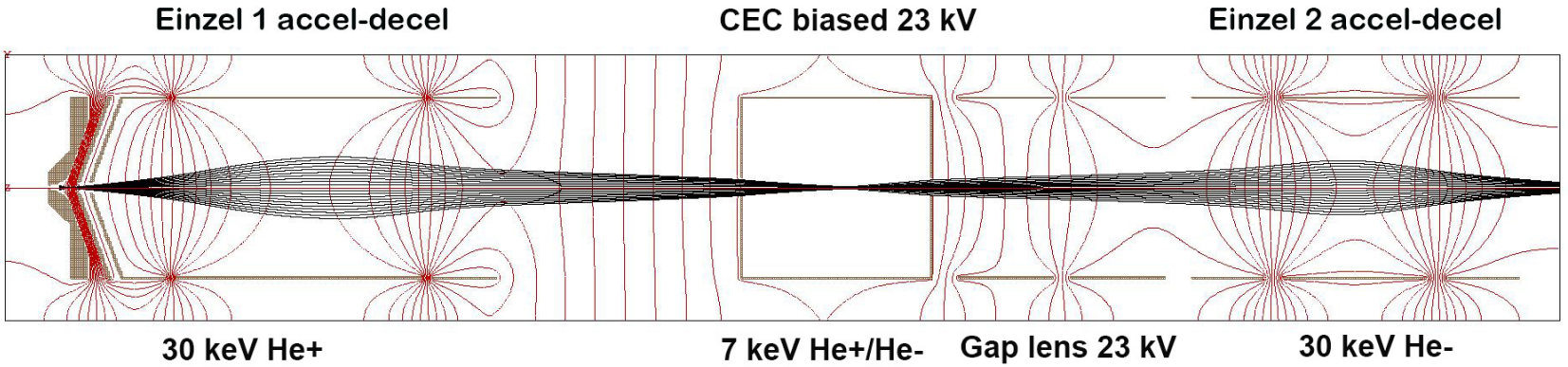
Interactions between low-energy ions and alkali vapor cause multiple Coulomb scattering. These collisions produce angular divergence on the milliradian scale and energy spreads of several hundred electron volts.

Normalized rms emittance of He^- beam from NEC Alphatross is 1.27 π mm mrad (80% of beam), Tesmer (1989). This is significant growth after passage CEC.

CRICOS PROVIDER #00120C

Beam Transport and Emittance Considerations





CRICOS PROVIDER #00120C

Diagnostics and Operational Reliability:
Beam, Plasma, and System Diagnostics

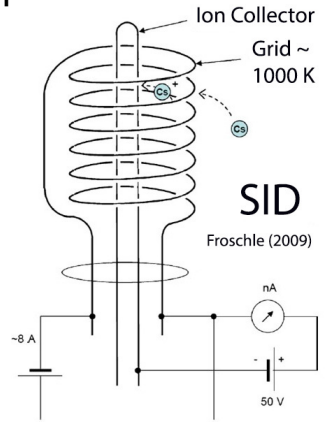
A suite of diagnostic tools is required for successful operation and/or optimization:

(a) Faraday cups, BPMs, emittance scanner for beam current, profile and quality. Individual Faraday cup should be able to measure fluxes of positive, neutral and negative particles. Also reported designs capable of measuring all three fluxes by reconfiguring operation of modified Faraday cup.

(b) RGA for residual gas composition

(c) Temperature sensors to control alkali vapor density

(d) Laser absorption spectroscopy or Langmuir surface ionization gauge to measure alkali vapor density, a quartz crystal microbalance to measure cumulative mass of alkali deposited on its surface



CRICOS PROVIDER #00120C

Diagnostics and Operational Reliability: *Contamination Control and Cleaning Methodologies*

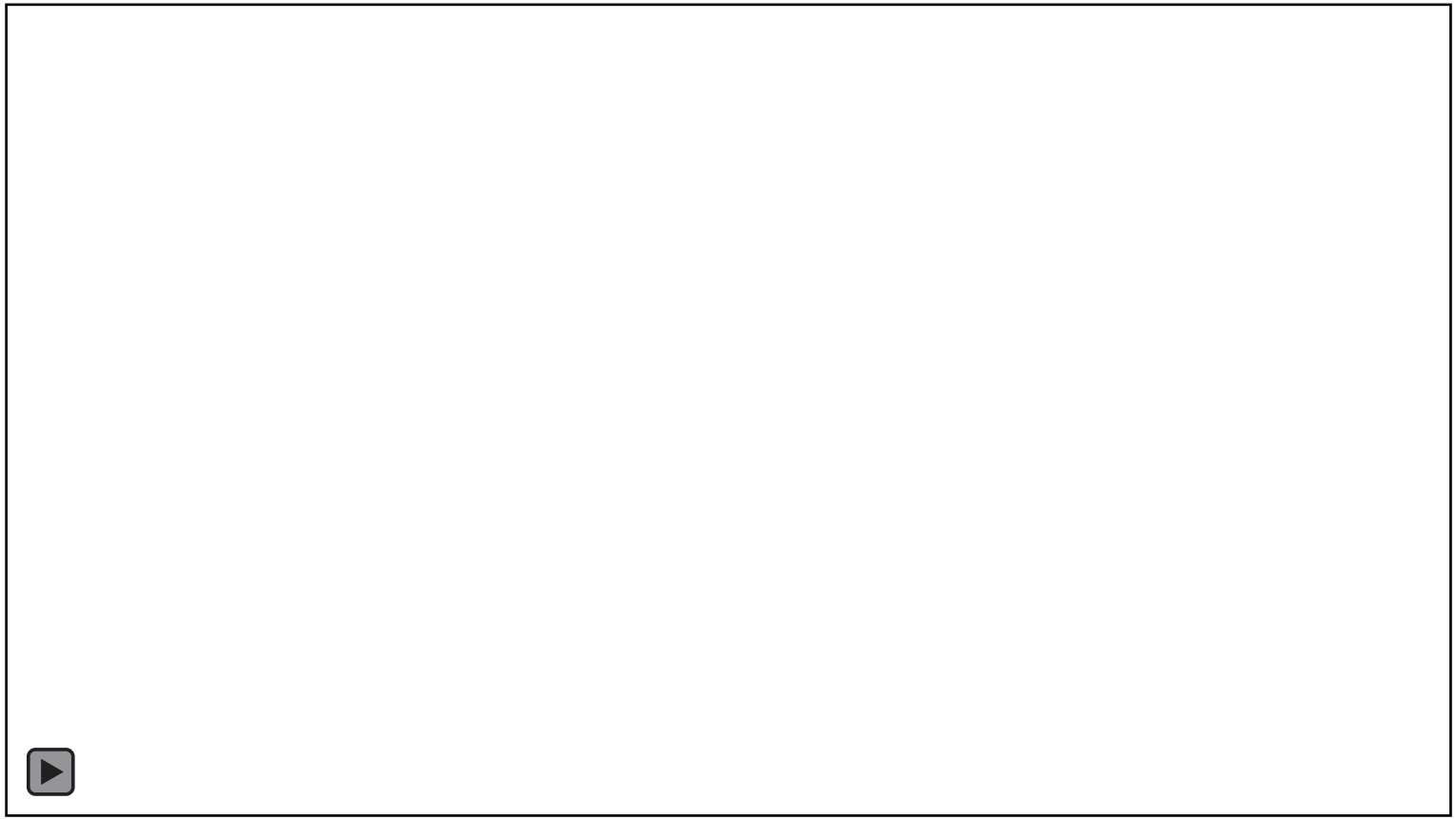
Major issues in real systems : (a) Cs/Rb react with residual air resulting in formation of almost solely into ionic compounds, highly corrosive substances such as the strongest water soluble base CsOH etc.; (b) introduced impurities O, N, C degrade overall performance.

The presence of oxygen has the most important role in corrosion of stainless steel and Ni-based alloys caused by Rb. The nuclear industry recommendation is to keep oxygen levels below 100 ppm in Rb- containing systems (storage of the radioactive isotope Kr-85).

Optimization of system performance is achieved by use of inert gas handling (Ar/N_2 purging); avoiding air exposure, contamination and selection of appropriate materials in the design such as stainless steel 316, nickel-plated surfaces and Nb alloys for ultimate performance. Thorough cleaning of vacuum system before operation is essential.

CRICOS PROVIDER #00120C

Alkali Free Charge-Exchange Media for He^- beams production

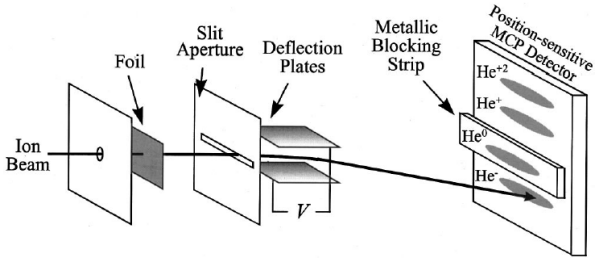


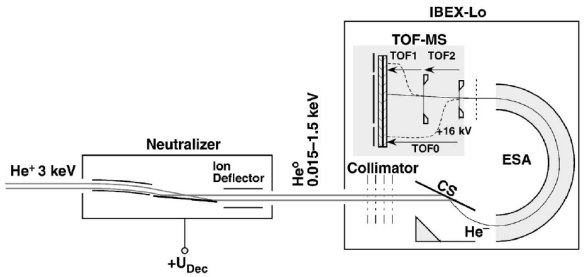
CRICOS PROVIDER #00120C

Alkali Free Charge-Exchange Media for He^- beams production

Negative ions have been produced by converting positively charged beams in gas charge-exchange cells; however, this method suffers from very low efficiency. For example, hydrogen gas yields a negative helium ion production efficiency of only ~10^{-5} , John et.al. (1967)

He^- ions have also been observed in the charge-state distributions of 8–80 keV He^+ ions transmitted through thin carbon foils (~1 $\mu g/cm^2$), Funsten (2001). At the optimum velocity (~$0.7v_0$, where v_0 is the Bohr velocity), the maximum He^- fraction reaches only 0.026%, significantly lower than that achieved with alkali targets.





He^- formation has also been observed during scattering of ground-state helium atoms from DLC-coated silicon surfaces, Wurtz (2008). For incident energies of 10–1500 eV, the negative ion fraction ranges from 7×10^{-5} to 10^{-5}. Because metastable He* lies energetically close to the He^- state, it may enhance He^- production by several orders of magnitude through surface charge-transfer processes.

CRICOS PROVIDER #00120C

Alkali Free Charge-Exchange Media for He^- beams production presented at NIBS 2026

Invited S1:
Negative Helium Ion Production Using Nano-Foils P. Jackle

Invited S1:
Alternative Solution to Address the Challenge of Negative Ion Sources for Fusion
L. Couedel

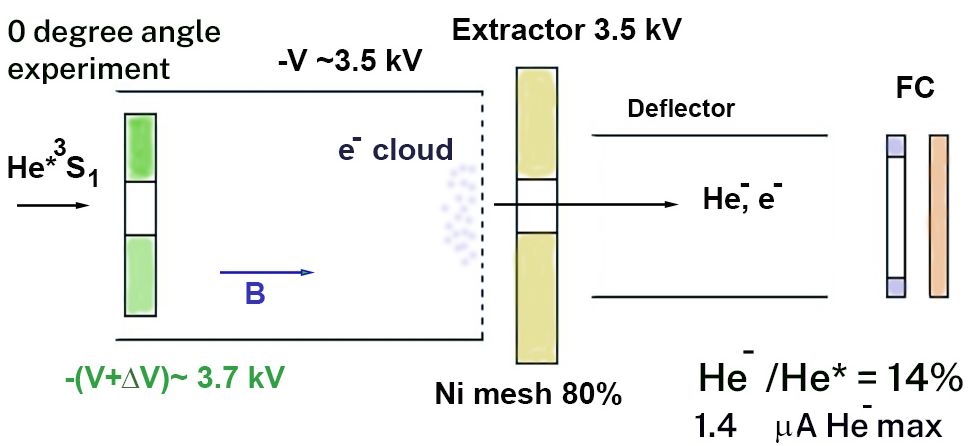
Poster session 1:
Alkali-Free Volume Production of He- Ions in Pure Helium Plasma: A Computational Modelling Framework S. Baghel, M. Dehnel et al

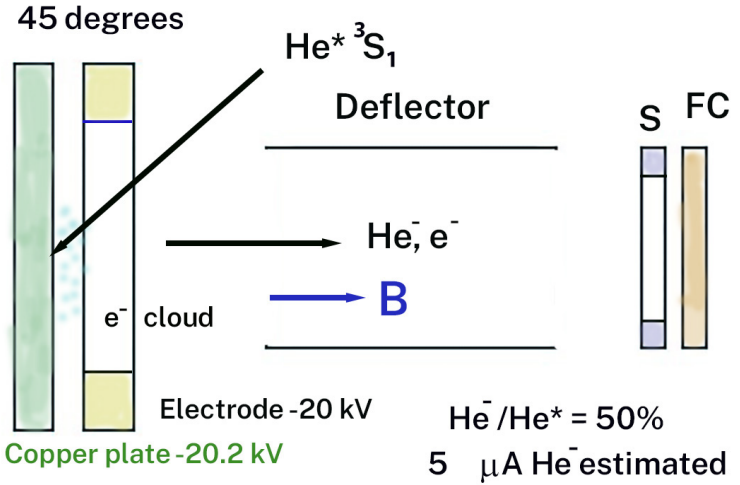
Invited S2:
Caesium Free Negative Ion Beam Developments using Microwave Heating of Low-Work Function Materials A. Matsubara

CRICOS PROVIDER #00120C

Beyond Alkali: Alternative Charge-Exchange Method for μA He^- beams

Direct production of He^- from metastable $He^*(2^3S_1)$ atoms via single-electron capture has been demonstrated, Law (1984). A gas-discharge source generates a dense metastable helium beam that passes through an electron-donor region, producing estimated He^- currents of up to 1.4 μA from a 10 μA metastable beam. Conversion efficiencies ~50% reported in a 45° geometry. The proposed mechanism involving capture from a trapped secondary-electron cloud remains debatable. Surface-assisted electron attachment may instead be the dominant formation pathway.



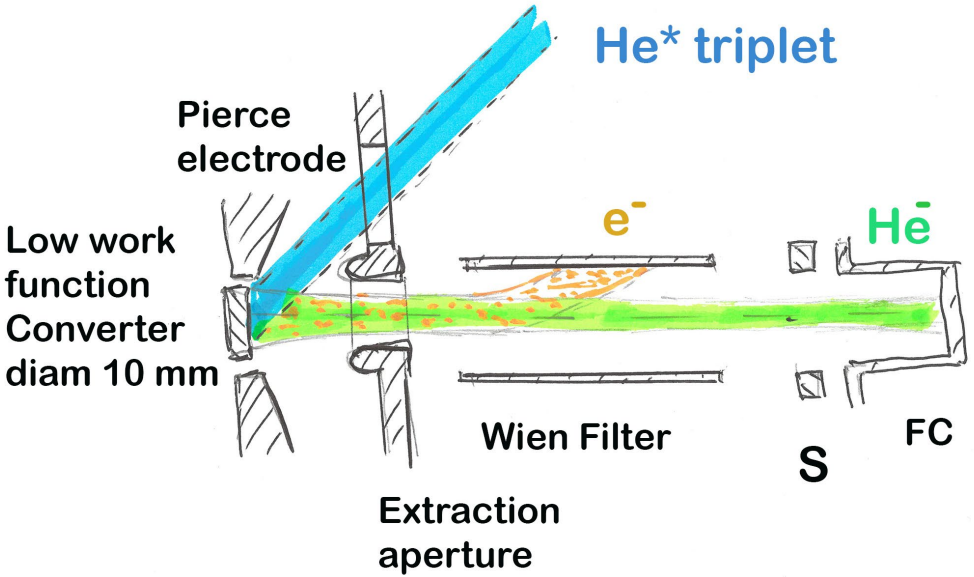


CRICOS PROVIDER #00120C

Production μA He^- beams at reduced Alkali Target Density

Proposed novel method of He^- formation in nearly alkali free environment.

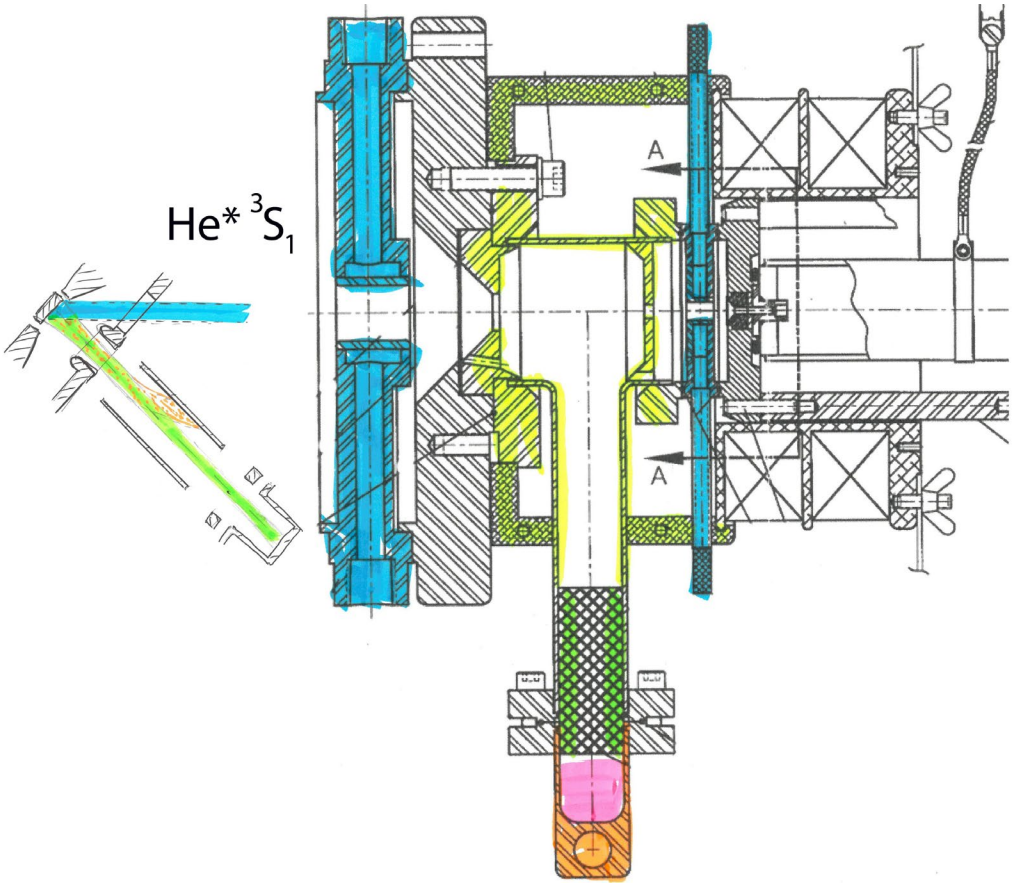
Metastable helium atoms He* can be generated by charge exchange in a Cs or Rb vapor cell with only trace amounts of alkali vapor, Rose et. al (1967).



Metastable helium atoms subsequently interact with low-work-function surfaces where resonant electron-transfer processes produce metastable He^- ions. Surface-assisted formation of He^- has been experimentally reported by Law et al. (1984)

CRICOS PROVIDER #00120C

Production μA He^- beams at reduced Alkali Target Density



CRICOS PROVIDER #00120C

Future Directions: Challenges Toward Alkali Free He^- Production

Promising research direction is the alkali free production of He^- through metastable-He* interactions with engineered surfaces such as low-work-function, nanostructures electron donor surfaces, diamond-like carbon coatings or two-dimensional materials and metamaterials.

Potential mechanisms of He^- formation include resonant surface charge transfer reaction and electron tunneling from low-work-function materials.

Key R&D challenges incorporate negative-ion survival probability, surface-state engineering, electron capture dynamics, surface degradation mechanisms and scalability for accelerator applications.

CRICOS PROVIDER #00120C

Conclusions and Outlook

1. Optimization of He^- output is multi-parameter problem involving interplay between beam energy, charge-exchange target thickness, alkali-vapor density, ion-source performance, vacuum conditions, and beam transport.

2. Maximum He^- beam current is achieved not through optimization of charge-exchange efficiency alone, but through simultaneous optimization of the injected He^+ beam intensity and the charge-exchange environment.

3. Importance is attributed to maintaining optimum alkali-vapor density, stable thermal conditions, low emittance beam formation/transport, and robust vacuum isolation.

4. Future developments may benefit from investigations of alkali-free conversion techniques based on metastable helium interactions with engineered low-work-function or nanostructured surfaces. Such approaches could potentially mitigate contamination and operational challenges associated with alkali-metal systems while opening new pathways toward compact and reliable He^- sources.

CRICOS PROVIDER #00120C

National Electrostatics Corp.

NCRIS
National Research Infrastructure for Australia
An Australian Government Initiative

HIA
HEAVY ION ACCELERATORS

CRICOS PROVIDER #00120C

THANK YOU

Contact Us

Heavy Ion Accelerator Facility
Australian National University
T +61 2 6125 2862
E Nikolai.Lobanov@anu.edu.au
W hiaf.anu.edu.au



Australian
National
University

CRICOS PROVIDER #00120C